CANCER GENOMICS & PROTEOMICS *19*: 584-590 (2022)
doi:10.21873/cgp.20343

Presence of a t(12;18)(q14;q21) Chromosome Translocation and Fusion of the Genes for High-mobility Group AT-Hook 2 (*HMGA2*) and WNT Inhibitory Factor 1 (*WIF1*) in Infrapatellar Fat Pad Cells from a Patient With Hoffa's Disease

IOANNIS PANAGOPOULOS[1], KRISTIN ANDERSEN[1], LUDMILA GORUNOVA[1], MARTINE EILERT-OLSEN[1], MARIUS LUND-IVERSEN[2], TRYGVE WESSEL-AAS[3], ISABEL LLORET[4], FRANCESCA MICCI[1] and SVERRE HEIM[1]

[1]*Section for Cancer Cytogenetics, Institute for Cancer Genetics and Informatics, The Norwegian Radium Hospital, Oslo University Hospital, Oslo, Norway;*
[2]*Department of Pathology, The Norwegian Radium Hospital, Oslo University Hospital, Oslo, Norway;*
[3]*Division of Orthopaedic Surgery, Oslo University Hospital, Oslo, Norway;*
[4]*Department of Radiology, The Norwegian Radium Hospital, Oslo University Hospital, Oslo, Norway*

Abstract. *Background/Aim: Hoffa's disease is anterior knee pain presumably stemming from inflammatory fibrous hyperplasia of the infrapatellar fat pad (Hoffa's pad). The etiology and pathogenesis are unclear, however, and no genetic information about the disease has been published. We report the genetic findings in cells from the fat pad of a patient with Hoffa's disease. Materials and Methods: Infrapatellar fat pad cells from a patient with Hoffa's disease were examined using cytogenetic, RNA sequencing, reverse transcription-polymerase chain reaction, and Sanger sequencing techniques. Results: Cytogenetic examination of short-term cultured cells from the Hoffa's pad revealed a balanced t(12;18)(q14;q21) translocation as the sole chromosomal aberration. RNA sequencing detected an out-of-frame fusion of exon 3 of the gene coding for high mobility group AT-hook 2 (HMGA2) with exon 9 of the gene coding for WNT inhibitory factor 1 (WIF1). The fusion was subsequently verified by reverse transcription-polymerase chain reaction together with Sanger sequencing. Conclusion: Our data indicate that Hoffa's disease is a neoplastic process with acquired genetic aberrations similar to those found in many benign tumors of connective tissues. The genetic aberrations are presumably acquired by mesenchymal stem cells of the infrapatellar fat pad inducing proliferation and differentiation into adipocytes or other mature connective tissue cells.*

Correspondence to: Ioannis Panagopoulos, Section for Cancer Cytogenetics, Institute for Cancer Genetics and Informatics, The Norwegian Radium Hospital, Oslo University Hospital, Montebello, PO Box 4954 Nydalen, NO-0424 Oslo, Norway. Tel: +47 22782362, email: ioannis.panagopoulos@rr-research.no

Key Words: Hoffa's disease, infrapatellar fat pad, cytogenetics, chromosome aberrations, *HMGA2, WIF1,* fusion gene, neoplasm.

In 1904, the German pathologist Albert Hoffa described an infrapatellar fat pad (later called Hoffa's pad) positioned just underneath the kneecap (patella), behind the patellar tendon and in front of the femoral condyles and tibial plateaus in patients with knee pain (1). The normal function of Hoffa's pad is still not known but it is probably important for normal knee kinematics (2-7). Histological examination of such infrapatellar fat pads shows a typical adipose tissue structure with mature fat cells making up most of the cell population (8-10). Infrapatellar fat pads have been shown to contain mesenchymal stem cells which, under specific culture conditions, can differentiate into different connective tissue elements such as chondrocytes, adipocytes, and osteoblasts (11-13). In Hoffa's disease, when the patient has anterior knee pain, the infrapatellar fat pad may be enlarged and display some degree of fibro-inflammatory admixture (1, 3, 9). Whether the dominant feature of such lesions is inflammation, hyperplasia, metaplasia or neoplasia, remains unknown.

We recently analyzed cytogenetically, as well as molecularly, cells from an infrapatellar fat pad removed from a patient with Hoffa's disease. Here we report the genetic findings characterizing that lesion.

Materials and Methods

Ethics statement. The study was approved by the Regional Ethics Committee (Regional komité for medisinsk forskningsetikk Sør-Øst, Norge, http://helseforskning.etikkom.no). All clinical information has been de-identified.

Case presentation. A 41-year-old man presented with a non-tender, hard and firm lesion at the lateral aspect of the patellar tendon which had increased in size over a period of 12 months. Knee discomfort was only mild and joint mobility was normal. The skin overlying the tumor was freely moveable upon palpation. Magnetic resonance imaging of the knee showed an expansive and ill-defined soft-tissue lesion in the infrapatellar fat pad, located just lateral and dorsal to the patellar tendon and measuring 4×4×3 cm (Figure 1). The lesion appeared heterogeneous, mainly with low T2-weighted signal and no contrast enhancement, suggesting hemosiderin deposits or fibrotic content (Figure 1A and B). Some areas showed high T2-weighted signal with no contrast enhancement, indicating cystic or myxoid components. Magnetic resonance imaging showed diffuse edema affecting Hoffa's fat pad in its entirety and the subcutaneous tissue immediately overlying the lesion (Figure 1C). Conventional X-ray examination showed no sign of mineralization in the lesion.

The preliminary diagnosis based on clinical and radiological findings was Hoffa's disease in chronic phase. There were no associated findings. Biopsy of the lesion showed fibrous and myxoid tissue without any sign of malignancy. After the biopsy procedure, the patient developed increasing pain in the knee, and for both diagnostic and therapeutic purposes, the lesion was surgically excised. Macroscopically, the lesion was white with well-defined borders. The surgical specimen was egg-shaped with a smooth surface but slightly whorled on cross section. Histological examination of the 37 mm diameter lesion revealed a chondromyxoid structure. The fibrous tissue in the periphery showed nodular proliferation and fascicles of spindle cells embedded in a chondromyxoid stroma. The tumor cells had vesicular nuclei with slight variation in size and shape. Mitotic figures or necrosis were not present. Tumor cells stained positive for S-100, as would be expected given their chondroid differentiation.

G-Banding and karyotyping. A part of the resected specimen was minced with scalpels into 1-2 mm fragments and then disaggregated with collagenase II (Worthington, Freehold, NJ, USA). The resulting cells were cultured, harvested, and processed for cytogenetic examination using standard techniques (14). G-Banding chromosome staining was achieved using Wright's stain (Sigma-Aldrich, St Louis, MO, USA) (14). Peripheral blood lymphocytes stimulated with phytohemagglutinin (PHA) for 72 h were karyotyped as a control. Metaphases were analyzed and karyograms prepared using the CytoVision computer-assisted karyotyping system (Leica Biosystems, Newcastle upon Tyne, UK). The karyotype was written according to the International System for Human Cytogenomic Nomenclature (15).

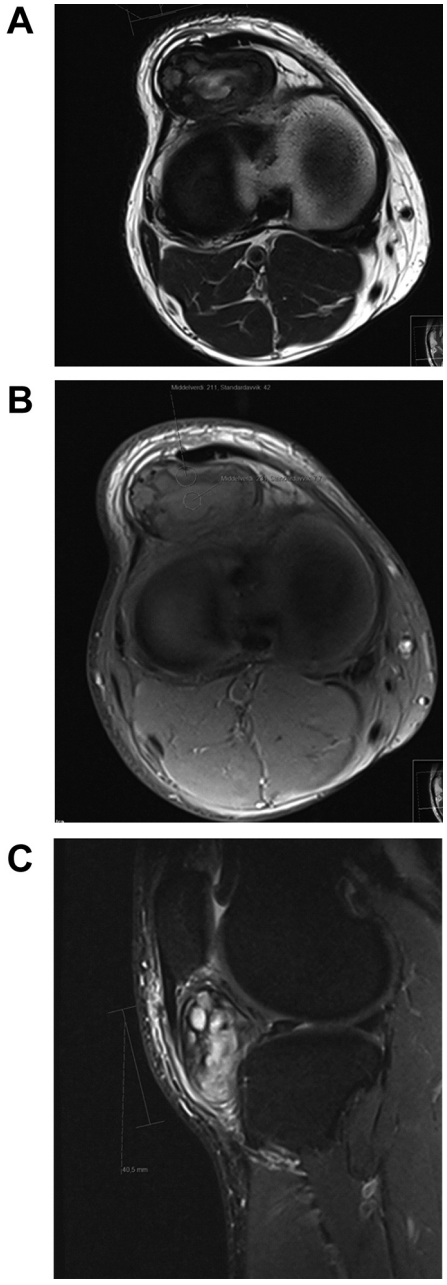

Figure 1. *Magnetic resonance imaging of the knee showing an expansive and ill-defined lesion in the infrapatellar fat pad consistent with Hoffa's disease. Axial T2-weighted (A) and axial T1 postcontrast fat-suppressed (B) images demonstrated a heterogeneous lesion with areas of T2 hypointensity and no contrast enhancement, suggesting fibrotic tissue or hemosiderin deposits, and areas with T2 hyperintensity with no contrast enhancement, indicating cystic or myxoid components. C: Sagittal short tau inversion recovery image revealed diffuse edema around the lesion involving the entire Hoffa fat pad and subcutaneous tissue.*

RNA sequencing. Total RNA was extracted using miRNeasy Mini Kit and QIAcube according to the manufacturer's instructions (Qiagen, Hilden, Germany) from tissue frozen and stored at −80˚C adjacent to

Table I. *Primers used for polymerase chain reaction amplification and Sanger sequencing analyses.*

Gene	Primer name	Primer sequence (5´->3´)	Reference sequence: Position	Chromosome band
ABL proto-oncogene 1, non-receptor tyrosine kinase	ABL1-91F1	CAG CGG CCA GTA GCA TCT GAC TTT G	NM_005157.4: 91-115	9q34.12
	ABL1-404R1	CTC AGC AGA TAC TCA GCG GCA TTG C	NM_005157.4: 428-404	9q34.12
High-mobility group AT-hook 2	HMGA2-982F1	CAA GAG TCC CTC TAA AGC AGC TCA	NM_003483.4: 982-1005	12q14.3
	HMGA2-1012F1	AGC AGA AGC CAC TGG AGA AAA AC	NM_003483.4: 1012-1034	12q14.3
WNT inhibitory factor 1	WIF1-1070R1	ATT TGT TGG GTT CAT GGC AGG	NM_007191.5: 1090-1070	12q14.3
	WIF1-1076R1	CAT TGG CAT TTG TTG GGT TCA T	NM_007191.5: 1097-1076	12q14.3

that used for cytogenetic analysis and histological examination. The tissue was disrupted and homogenized in Qiazol Lysis Reagent (Qiagen) with 5 mm stainless steel beads and TissueLyser II (Qiagen). Subsequently, total RNA was purified using QIAcube (Qiagen). The RNA quality was evaluated with a 2100 Bioanalyzer system and RNA 6000 Nano Kit (Agilent, Santa Clara, CA, USA). One microgram of total RNA was sent to the Genomics Core Facility at the Norwegian Radium Hospital, Oslo University Hospital for high-throughput paired-end RNA sequencing. A total of 123 million reads of 101-bp length were obtained. FASTQC software was used for quality control of the raw sequence data (available online at: http://www.bioinformatics.babraham.ac.uk/projects/fastqc/). Fusion transcripts were found using FusionCatcher software (16, 17).

Reverse transcription-polymerase chain reaction (RT-PCR) and Sanger sequencing analyses. The primers for the genes ABL proto-oncogene 1, non-receptor tyrosine kinase (*ABL1*), high mobility group AT-hook 2 (*HMGA2*), and WNT inhibitory factor 1 (*WIF1*) are described in Table I. Complementary DNA (cDNA) was synthesized from 1 μg of total RNA in a 20-μl reaction volume using iScript Advanced cDNA Synthesis Kit for RT-qPCR according to the manufacturer's instructions (Bio-Rad, Hercules, CA, USA). cDNA corresponding to 20 ng total RNA was then used as template in a 25-μl reaction volume PCR assay containing 12.5 μl Premix Ex Taq™ DNA Polymerase Hot Start Version (Takara Bio Europe/SAS, Saint-Germain-en-Laye, France) and 0.4 μM of each of the forward and reverse primers (Table I). The primer combination ABL1-91F1/ABL1-404R1 was used to amplify a 338 bp cDNA fragment from the *ABL1* gene in order to check the quality of cDNA synthesis. To detect the *HMGA2::WIF1* fusion transcript (see below), the primer combinations HMGA2-1012F1/WIF1-1070R1 and HMGA2-982F1/WIF1-1076R1 were used. A C-1000 Thermal cycler (Bio-Rad) was used for PCR amplifications. The cycling profile was 30 s at 94˚C followed by 35 cycles of 7 s at 98˚C, 30 s at 60˚C, 30 s at 72˚C, and a final extension step for 5 min at 72˚C. Three microliters of the PCR products were stained with GelRed (Biotium, Fremont, CA, USA), analyzed by electrophoresis through 1.0% agarose gel, and photographed. Gel electrophoresis was performed using lithium borate buffer (18). The remaining PCR products were purified using the MinElute PCR Purification Kit (Qiagen) and Sanger sequenced with the dideoxy procedure using the BigDye Direct Cycle Sequencing Kit in accordance with the company's recommendations (ThermoFisher Scientific, Waltham, MA, USA). The primers used for sequencing were the same as those used for PCR with addition of M13 forward and M13 reverse sequences at their 5´-ends. The forward primers HMGA2-1012F1 and HMGA2-982F1 contained M13 forward sequence at their 5´-end (TGTAAAACGACGGCCAGT) whereas the reverse WIF1-1070R1 and WIF1-1076R1 primers contained the M13 reverse primer sequence at their 5´-end (CAGGAAACAGCTATGACC). Sequencing was run on the Applied Biosystems SeqStudio Genetic Analyzer system (ThermoFisher Scientific). The basic local alignment search tool (BLAST) was used to compare the sequences obtained by Sanger sequencing with the NCBI reference sequences NM_003483.4 (*HMGA2*) and NM_007191.5 (*WIF1*) (19).

Results

Cytogenetic examination of short-term cultured cells from the infrapatellar fat pad revealed a balanced t(12;18)(q14;q21) translocation as the sole chromosome aberration in all examined metaphases (Figure 2). Consequently, the karyotype of the lesion was 46,XY,t(12;18)(q14;q21)[10]. At the same time, G-banding analysis of PHA-stimulated peripheral blood cells yielded a normal 46,XY karyotype. Thus, the translocation t(12;18)(q14;q21) was an acquired cytogenetic abnormality found only in cells of the infrapatellar fat pad.

Analysis of raw sequencing data using FusionCatcher detected a fusion of exon 3 of *HMGA2* from 12q14.3 (nucleotide 1060 in the NCBI reference sequences NM_003483.4) with exon 9 of *WIF1* from 12q14.3 (nucleotide 1037 in reference sequence NM_007191.5): AGCCACTGGAGAAAAACGGCCAAGAGGCAGACCTA GGAAATGG-CTGTCTGCGAGCCTGGCTGTGGTG CACATGGAACCTGCCATGA. To verify the *HMGA2::WIF1* fusion transcript obtained by RNA sequencing, PCR amplifications were performed with two forward *HMGA2* and two reverse *WIF1* primers corresponding to sequences upstream and downstream of the putative fusion point, respectively. RT-PCR with primer combinations HMGA2-1012F1/WIF1-1070R1 and HMGA2-982F1/WIF1-1076R1 amplified 103-bp and 150-bp cDNA fragments, respectively, strongly suggesting the presence of a *HMGA2::WIF1* fusion transcript (Figure 3A). Sanger sequencing of both amplified cDNA fragments showed that they were *HMGA2::WIF1* fusion transcripts with a fusion point identical to that found by RNA sequencing (Figure 3B).

Figure 2. *Cytogenetic analysis of the specimen obtained from the surgically removed Hoffa's fat pad. The karyogram shows the t(12;18)(q14;q21) chromosomal translocation as the sole cytogenetic abnormality. Breakpoint positions are indicated by arrows.*

The fusion transcript is predicted to be out-of-frame coding for a 124 amino acid-long protein composed of the first 82 amino acids of HMGA2 and 42 amino acids encoded by the *WIF1* sequence (Figure 2C). The 42 amino acids of the latter do not correspond to any known protein, nor do they contain known motifs or domains.

Discussion

Our data strongly indicate that Hoffa's disease – or rather the knee lesion known as Hoffa's fat pad – is a neoplastic process. Central to this conclusion was the finding of a clonal chromosomal translocation, t(12;18)(q14;q21), as an acquired cytogenetic aberration in Hoffa's pad cells (whereas analysis of PHA-stimulated peripheral blood cells yielded a normal 46,XY karyotype). With very few exceptions, for example trisomy 7 in solid tissue lesions (20), the general rule is that whenever acquired clonal chromosomal abnormalities are found in an investigated disease process, this means that the disease is neoplastic (21). Furthermore, but equally important, a similar t(12;18)(q14~15;q12~21) translocation has been reported before as the sole karyotypic aberration in lipomas (22).

Secondly, the detection of an *HMGA2::WIF1* fusion transcript in cells cultured from the lesion strongly supports the conclusion that Hoffa's disease is a neoplastic one, or at least that was so in the patient we examined, the only analysis of a Hoffa's pad we have ever undertaken. An *HMGA2::WIF1* fusion transcript was also reported in salivary gland pleomorphic adenomas (23-26), in a breast adenomyoepithelioma (27), and in a pleomorphic adenoma of the breast (28). In other words, *HMGA2::WIF1* fusion transcripts are associated with neoplastic processes, more specifically with benign tumors. Various alternative *HMGA2::WIF1* chimeric transcripts have been reported, and the transcript found in a pleomorphic adenoma of the salivary gland was identical to the transcript we describe here, *i.e.* it had fusion of exon 3 from *HMGA2* with exon 9 from *WIF1* [sequence with accession number EU263622, case 6 in (24)].

Both the *HMGA2* and *WIF1* genes map to chromosome subband 12q14.3. The genomic distance between them is 0.7 Mbp but they are transcribed in opposite directions. Thus, we surmise that a submicroscopic inversion occurred together with the 12q14;18q21-translocation generating the observed *HMGA2::WIF1* fusion gene. The situation would be similar to what was found in a lipoma carrying a t(12;18)(q14~q15;q12~q21) together with a fusion of

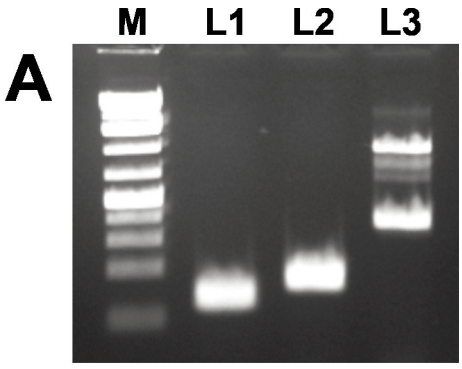

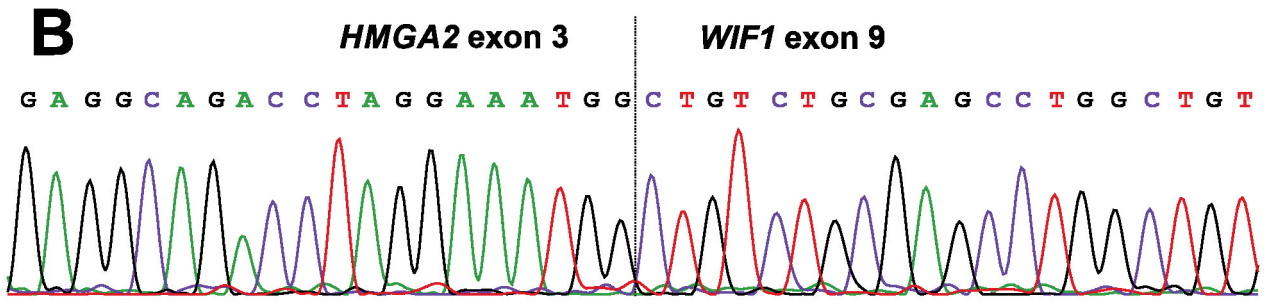

C

```
atg agc gca cgc ggt gag ggc gcg ggg cag ccg tcc act tca gcc cag gga caa cct gcc
 M   S   A   R   G   E   G   A   G   Q   P   S   T   S   A   Q   G   Q   P   A
gcc cca gcg cct cag aag aga gga cgc ggc cgc ccc agg aag cag cag caa gaa cca acc
 A   P   A   P   Q   K   R   G   R   G   R   P   R   K   Q   Q   Q   E   P   T
ggt gag ccc tct cct aag aga ccc agg gga aga ccc aaa ggc agc aaa aac aag agt ccc
 G   E   P   S   P   K   R   P   R   G   R   P   K   G   S   K   N   K   S   P
tct aaa gca gct caa aag aaa gca gaa gcc act gga gaa aaa cgg cca aga ggc aga cct
 S   K   A   A   Q   K   K   A   E   A   T   G   E   K   R   P   R   G   R   P
agg aaa tgg ctg tct gcg agc ctg gct gtg gtg cac atg gaa cct gcc atg aac cca aca
 R   K   W   L   S   A   S   L   A   V   V   H   M   E   P   A   M   N   P   T
aat gcc aat gtc aag aag gtt ggc atg gaa gac act gca ata aaa ggt acg aag cca gcc
 N   A   N   V   K   K   V   G   M   E   D   T   A   I   K   G   T   K   P   A
tca tac atg ccc tga
 S   Y   M   P   -
```

Figure 3. *Molecular genetic examination of the specimen obtained from the surgically removed fat pad of a patients with Hoffa's disease. A: Gel electrophoresis showing the amplified cDNA fragments obtained with reverse transcription polymerase chain reaction for high-mobility group AT-hook 2 (HMGA2) and WNT-inhibitory factor 1 (WIF1) genes using the primer combinations HMGA2-1012F1/WIF1-1070R1 (L1), HMGA2-982F1/WIF1-1076R1 (L2), and ABL1-91F1/ABL1-404R1 (L3). M: GeneRuler 1 kb Plus DNA ladder (ThermoFisher Scientific). B: Partial sequence chromatograms of the cDNA amplified fragment showing the junction position of HMGA2 and WIF1 (vertical dotted line). C: The coding part of the HMGA2::WIF1 fusion transcript and the putative 124 amino acid-long HMGA2 peptide containing amino acid residues 1-82 from HMGA2 (accession number NP_003474.1) corresponding to exons 1-3 of that gene, and 42 amino acid residues from the WIF1 sequence. The 42 amino acid sequence does not correspond to any known protein nor does it have known motifs and domains. The three AT-hook domains of HMGA2 are shown in bold red letters.*

HMGA2 with the glutamate receptor interacting protein 1 (*GRIP1*) gene (22). *GRIP1* also maps to chromosome subband 12q14.3 and is transcribed in the opposite direction from *HMGA2*.

The consequence of the *HMGA2::WIF1* fusion we describe is similar to that of many other *HMGA2* rearrangements found in various benign connective tissue tumors and discussed in several previous publications (22, 29-31). In

brief, the 3´-untranslated region of *HMGA2* (3´-UTR) strongly represses the expression of *HMGA2* (32). The 3´-UTR of *HMGA2* contains many regulatory elements (33), seven or eight of which target sites for the miRNA *let-7* that suppresses *HMGA2* expression in normal nonembryonic tissues (34, 35). Disruption of the *HMGA2* locus separates exons 1-3 (or exons 1-4) from the 3´-UTR. As a consequence, the part of *HMGA2* which codes for the three AT-hook binding domains (exons 1-3) becomes overexpressed and thus acts to transform the cell neoplastically. This transforming potential of truncated *HMGA2* in the development of neoplasias has been repeatedly demonstrated (36-42).

In conclusion, our data indicate that the abnormal fat pad of Hoffa's disease is not a simple inflammatory fibrous hyperplasia of infrapatellar fat cells but rather a neoplasm with acquired genetic aberrations similar to those found in many benign tumors. The genetic aberrations probably occur in mesenchymal stem cells of the infrapatellar fat pad and may induce proliferation and differentiation into adipocytes as well as other connective tissue cells, including chondrocytes and osteoblasts.

Conflicts of Interest

The Authors declare that they have no potential conflicts of interest.

Authors' Contributions

IP designed and supervised the research, performed molecular genetic experiments and bioinformatics analysis, and wrote the article. KA performed molecular genetic experiments and evaluated the data. LG performed cytogenetic analysis. ME-O evaluated the cytogenetic results. ML-I performed the pathological examination. TW-A made the diagnosis and surgically removed the lesion. IL performed the radiological examination. FM evaluated the data. SH assisted with experimental design and writing of the article. All Authors read and approved the final article.

Acknowledgements

This work was supported by grants from Radiumhospitalets Legater.

References

1 Hoffa A: The influence of the adipose tissue with regard to the pathology of the knee joint. JAMA: The Journal of the American Medical Association *XLIII(12)*: 795, 2016. DOI: 10.1001/jama.1904.92500120002h

2 Bohnsack M, Wilharm A, Hurschler C, Rühmann O, Stukenborg-Colsman C and Wirth CJ: Biomechanical and kinematic influences of a total infrapatellar fat pad resection on the knee. Am J Sports Med *32(8)*: 1873-1880, 2004. PMID: 15572315. DOI: 10.1177/0363546504263946

3 Eymard F and Chevalier X: Inflammation of the infrapatellar fat pad. Joint Bone Spine *83(4)*: 389-393, 2016. PMID: 27068617. DOI: 10.1016/j.jbspin.2016.02.016

4 Jarraya M, Diaz LE, Roemer FW, Arndt WF, Goud AR and Guermazi A: MRI findings consistent with peripatellar fat pad impingement: How much related to patellofemoral maltracking? Magn Reson Med Sci *17(3)*: 195-202, 2018. PMID: 28993563. DOI: 10.2463/mrms.rev.2017-0063

5 Stephen JM, Sopher R, Tullie S, Amis AA, Ball S and Williams A: The infrapatellar fat pad is a dynamic and mobile structure, which deforms during knee motion, and has proximal extensions which wrap around the patella. Knee Surg Sports Traumatol Arthrosc *26(11)*: 3515-3524, 2018. PMID: 29679117. DOI: 10.1007/s00167-018-4943-1

6 Leese J and Davies DC: An investigation of the anatomy of the infrapatellar fat pad and its possible involvement in anterior pain syndrome: a cadaveric study. J Anat *237(1)*: 20-28, 2020. PMID: 32159227. DOI: 10.1111/joa.13177

7 Okita Y, Oba H, Miura R, Morimoto M and Gamada K: Movement and volume of infrapatellar fat pad and knee kinematics during quasi-static knee extension at 30 and 0˚ flexion in young healthy individuals. Knee *27(1)*: 71-80, 2020. PMID: 31918962. DOI: 10.1016/j.knee.2019.10.019

8 Macchi V, Porzionato A, Sarasin G, Petrelli L, Guidolin D, Rossato M, Fontanella CG, Natali A and De Caro R: The infrapatellar adipose body: a histotopographic study. Cells Tissues Organs *201(3)*: 220-231, 2016. PMID: 26796341. DOI: 10.1159/000442876

9 Mace J, Bhatti W and Anand S: Infrapatellar fat pad syndrome: a review of anatomy, function, treatment and dynamics. Acta Orthop Belg *82(1)*: 94-101, 2016. PMID: 26984660.

10 Macchi V, Stocco E, Stecco C, Belluzzi E, Favero M, Porzionato A and De Caro R: The infrapatellar fat pad and the synovial membrane: an anatomo-functional unit. J Anat *233(2)*: 146-154, 2018. PMID: 29761471. DOI: 10.1111/joa.12820

11 Wickham MQ, Erickson GR, Gimble JM, Vail TP and Guilak F: Multipotent stromal cells derived from the infrapatellar fat pad of the knee. Clin Orthop Relat Res *(412)*: 196-212, 2003. PMID: 12838072. DOI: 10.1097/01.blo.0000072467.53786.ca

12 Hindle P, Khan N, Biant L and Péault B: The infrapatellar fat pad as a source of perivascular stem cells with increased chondrogenic potential for regenerative medicine. Stem Cells Transl Med *6(1)*: 77-87, 2017. PMID: 28170170. DOI: 10.5966/sctm.2016-0040

13 Bravo B, Argüello JM, Gortazar AR, Forriol F and Vaquero J: Modulation of gene expression in infrapatellar fat pad-derived mesenchymal stem cells in osteoarthritis. Cartilage *9(1)*: 55-62, 2018. PMID: 29156945. DOI: 10.1177/1947603516686144

14 Mandahl N: Methods in solid tumour cytogenetics. In: Human Cytogenetics: Malignancy and Acquired Abnormalities. Rooney DE (ed.). New York, Oxford University Press, pp. 165-203, 2001.

15 McGowan-Jordan J, Simons A and Schmid M: ISCN 2016: An International System for Human Cytogenomic Nomenclature. Basel, Karger, pp. 140, 2016.

16 Kangaspeska S, Hultsch S, Edgren H, Nicorici D, Murumägi A and Kallioniemi O: Reanalysis of RNA-sequencing data reveals several additional fusion genes with multiple isoforms. PLoS One *7(10)*: e48745, 2012. PMID: 23119097. DOI: 10.1371/journal.pone.0048745

17 Nicorici D, Satalan H, Edgren H, Kangaspeska S, Murumagi A, Kallioniemi O, Virtanen S and Kikku O: FusionCatcher - a tool for finding somatic fusion genes in paired-end RNA-sequencing data. bioRxiv, 2014. DOI: 10.1101/011650

18 Singhal H, Ren YR and Kern SE: Improved DNA electrophoresis in conditions favoring polyborates and lewis acid complexation. PLoS One *5(6)*: e11318, 2010. PMID: 20593002. DOI: 10.1371/journal.pone.0011318

19 Altschul SF, Gish W, Miller W, Myers EW and Lipman DJ: Basic local alignment search tool. J Mol Biol *215(3)*: 403-410, 1990. PMID: 2231712. DOI: 10.1016/S0022-2836(05)80360-2

20 Johansson B, Heim S, Mandahl N, Mertens F and Mitelman F: Trisomy 7 in nonneoplastic cells. Genes Chromosomes Cancer *6(4)*: 199-205, 1993. PMID: 7685621. DOI: 10.1002/gcc.2870060402

21 Heim S and Mitelman F: Cancer cytogenetics: Chromosomal and molecular genetic abberations of tumor cells. Fourth Edition. Wiley-Blackwell, 2015.

22 Panagopoulos I, Gorunova L, Bjerkehagen B, Lobmaier I and Heim S: The recurrent chromosomal translocation t(12;18)(q14~15;q12~21) causes the fusion gene HMGA2-SETBP1 and HMGA2 expression in lipoma and osteochondrolipoma. Int J Oncol *47(3)*: 884-890, 2015. PMID: 26202160. DOI: 10.3892/ijo.2015.3099

23 Queimado L, Lopes CS and Reis AM: WIF1, an inhibitor of the Wnt pathway, is rearranged in salivary gland tumors. Genes Chromosomes Cancer *46(3)*: 215-225, 2007. PMID: 17171686. DOI: 10.1002/gcc.20402

24 Persson F, Andrén Y, Winnes M, Wedell B, Nordkvist A, Gudnadottir G, Dahlenfors R, Sjögren H, Mark J and Stenman G: High-resolution genomic profiling of adenomas and carcinomas of the salivary glands reveals amplification, rearrangement, and fusion of HMGA2. Genes Chromosomes Cancer *48(1)*: 69-82, 2009. PMID: 18828159. DOI: 10.1002/gcc.20619

25 Matsuyama A, Hisaoka M, Nagao Y and Hashimoto H: Aberrant PLAG1 expression in pleomorphic adenomas of the salivary gland: a molecular genetic and immunohistochemical study. Virchows Arch *458(5)*: 583-592, 2011. PMID: 21394649. DOI: 10.1007/s00428-011-1063-4

26 Agaimy A, Ihrler S, Baněčková M, Costés Martineau V, Mantsopoulos K, Hartmann A, Iro H, Stoehr R and Skálová A: HMGA2-WIF1 rearrangements characterize a distinctive subset of salivary pleomorphic adenomas with prominent trabecular (canalicular adenoma-like) morphology. Am J Surg Pathol *46(2)*: 190-199, 2022. PMID: 34324456. DOI: 10.1097/PAS.0000000000001783

27 Pareja F, Geyer FC, Brown DN, Sebastião APM, Gularte-Mérida R, Li A, Edelweiss M, Da Cruz Paula A, Selenica P, Wen HY, Jungbluth AA, Varga Z, Palazzo J, Rubin BP, Ellis IO, Brogi E, Rakha EA, Weigelt B and Reis-Filho JS: Assessment of *HMGA2* and *PLAG1* rearrangements in breast adenomyoepitheliomas. NPJ Breast Cancer *5*: 6, 2019. PMID: 30675516. DOI: 10.1038/s41523-018-0101-7

28 Pareja F, Da Cruz Paula A, Gularte-Mérida R, Vahdatinia M, Li A, Geyer FC, da Silva EM, Nanjangud G, Wen HY, Varga Z, Brogi E, Rakha EA, Weigelt B and Reis-Filho JS: Pleomorphic adenomas and mucoepidermoid carcinomas of the breast are underpinned by fusion genes. NPJ Breast Cancer *6*: 20, 2020. PMID: 32550265. DOI: 10.1038/s41523-020-0164-0

29 Panagopoulos I, Bjerkehagen B, Gorunova L, Taksdal I and Heim S: Rearrangement of chromosome bands 12q14~15 causing HMGA2-SOX5 gene fusion and HMGA2 expression in extraskeletal osteochondroma. Oncol Rep *34(2)*: 577-584, 2015. PMID: 26043835. DOI: 10.3892/or.2015.4035

30 Panagopoulos I, Gorunova L, Agostini A, Lobmaier I, Bjerkehagen B and Heim S: Fusion of the HMGA2 and C9orf92 genes in myolipoma with t(9;12)(p22;q14). Diagn Pathol *11*: 22, 2016. PMID: 26857357. DOI: 10.1186/s13000-016-0472-8

31 Panagopoulos I, Gorunova L, Andersen HK, Pedersen TD, Lømo J, Lund-Iversen M, Micci F and Heim S: Genetic characterization of myoid hamartoma of the breast. Cancer Genomics Proteomics *16(6)*: 563-568, 2019. PMID: 31659109. DOI:10.21873/cgp.20158

32 Borrmann L, Wilkening S and Bullerdiek J: The expression of HMGA genes is regulated by their 3'UTR. Oncogene *20(33)*: 4537-4541, 2001. PMID: 11494149. DOI: 10.1038/sj.onc.1204577

33 Kristjánsdóttir K, Fogarty EA and Grimson A: Systematic analysis of the Hmga2 3' UTR identifies many independent regulatory sequences and a novel interaction between distal sites. RNA *21(7)*: 1346-1360, 2015. PMID: 25999317. DOI: 10.1261/rna.051177.115

34 Lee YS and Dutta A: The tumor suppressor microRNA let-7 represses the HMGA2 oncogene. Genes Dev *21(9)*: 1025-1030, 2007. PMID: 17437991. DOI: 10.1101/gad.1540407

35 Mayr C, Hemann MT and Bartel DP: Disrupting the pairing between let-7 and Hmga2 enhances oncogenic transformation. Science *315(5818)*: 1576-1579, 2007. PMID: 17322030. DOI: 10.1126/science.1137999

36 Fedele M, Berlingieri MT, Scala S, Chiariotti L, Viglietto G, Rippel V, Bullerdiek J, Santoro M and Fusco A: Truncated and chimeric HMGI-C genes induce neoplastic transformation of NIH3T3 murine fibroblasts. Oncogene *17(4)*: 413-418, 1998. PMID: 9696033. DOI: 10.1038/sj.onc.1201952

37 Arlotta P, Tai AK, Manfioletti G, Clifford C, Jay G and Ono SJ: Transgenic mice expressing a truncated form of the high mobility group I-C protein develop adiposity and an abnormally high prevalence of lipomas. J Biol Chem *275(19)*: 14394-14400, 2000. PMID: 10747931. DOI: 10.1074/jbc.m000564200

38 Fedele M, Battista S, Kenyon L, Baldassarre G, Fidanza V, Klein-Szanto AJ, Parlow AF, Visone R, Pierantoni GM, Outwater E, Santoro M, Croce CM and Fusco A: Overexpression of the HMGA2 gene in transgenic mice leads to the onset of pituitary adenomas. Oncogene *21(20)*: 3190-3198, 2002. PMID: 12082634. DOI: 10.1038/sj.onc.1205428

39 Zaidi MR, Okada Y and Chada KK: Misexpression of full-length HMGA2 induces benign mesenchymal tumors in mice. Cancer Res *66(15)*: 7453-7459, 2006. PMID: 16885341. DOI: 10.1158/0008-5472.CAN-06-0931

40 Richter A, Lübbing M, Frank HG, Nolte I, Bullerdiek JC and von Ahsen I: High-mobility group protein HMGA2-derived fragments stimulate the proliferation of chondrocytes and adipose tissue-derived stem cells. Eur Cell Mater *21*: 355-363, 2011. PMID: 21484705. DOI: 10.22203/ecm.v021a26

41 Li Z, Gilbert JA, Zhang Y, Zhang M, Qiu Q, Ramanujan K, Shavlakadze T, Eash JK, Scaramozza A, Goddeeris MM, Kirsch DG, Campbell KP, Brack AS and Glass DJ: An HMGA2-IGF2BP2 axis regulates myoblast proliferation and myogenesis. Dev Cell *23(6)*: 1176-1188, 2012. PMID: 23177649. DOI: 10.1016/j.devcel.2012.10.019

42 Mas A, Cervelló I, Fernández-Álvarez A, Faus A, Díaz A, Burgués O, Casado M and Simón C: Overexpression of the truncated form of High Mobility Group A proteins (HMGA2) in human myometrial cells induces leiomyoma-like tissue formation. Mol Hum Reprod *21(4)*: 330-338, 2015. PMID: 25542836. DOI: 10.1093/molehr/gau114

Received May 3, 2022
Revised May 28, 2022
Accepted June 5, 2022